

# Adsorption of Conditioning Polymers on Solid Substrates with Different Charge Density

Eduardo Guzmán,<sup>†,‡</sup> Francisco Ortega,<sup>†</sup> Nawel Baghdadli,<sup>§</sup> Colette Cazeneuve,<sup>§</sup> Gustavo S. Luengo,<sup>\*,§</sup> and Ramón G. Rubio<sup>\*,†</sup>

<sup>†</sup>Departamento de Química Física I, Facultad de Ciencias Químicas, Universidad Complutense de Madrid, Ciudad Universitaria s/n, 28040-Madrid, Spain

<sup>§</sup>L'Oréal Research and Innovation, Aulnay-Sous Bois, France

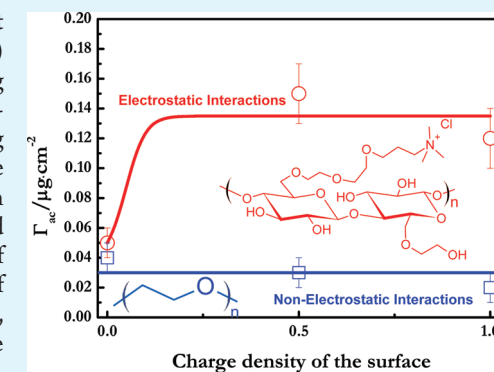
**ABSTRACT:** The adsorption processes of polymers that belong to two different families (neutral hydrophilic polymers and cationic polysaccharide polymers) onto solid surfaces with different charge density have been studied using dissipative quartz crystal microbalance (D-QCM) and ellipsometry. The polymers studied are very frequently used in the cosmetic industry as conditioning agents. The adsorption kinetics of the polymers involves at least two steps. The total adsorbed amount depends on the charge density of the surface for both types of polymers. The comparison of the adsorbed mass on each layer obtained from D-QCM and from ellipsometry has allowed calculating the water content of the layers that reaches high values for the polymers studied. The analysis of D-QCM results also provided information about the shear modulus of the layers, whose values have been found to be typical of a rubber-like polymer system. The main driving force of the adsorption was found to be the energy of the interactions between chains and surface.

**KEYWORDS:** polymers, charge density, solid surface, D-QCM, ellipsometry

## 1. INTRODUCTION

The interaction between macromolecules (synthetic polymers, polyelectrolytes or proteins) and interfaces, solid<sup>1</sup> or fluid,<sup>2,3</sup> is a field that has attracted much attention in the last years with noticeable theoretical and experimental advances.<sup>4–8</sup> Polymer adsorption onto surfaces strongly modifies the properties and interactions of the surfaces, and therefore is an important issue in many technological applications involving polymer thin coatings, such as: biocompatible coatings, stabilization of colloidal solutions and particles dispersions, flocculation process, surface treatment, cosmetics (e.g., hair conditioners), and in general, in a large number of areas in the field of nanotechnologies.<sup>9</sup>

One of the fields where the interactions between macromolecules and surfaces are very important is for the fabrication of hair care products where different kinds of macromolecules are incorporated to meet a variety of requirements.<sup>10</sup> Shampoos and conditioners are widely used to clean and improve the sensorial properties of the fibers. These products, mostly used in a water medium, rely on the deposition of polymers on a relatively big effective surface (c.a.  $6 \text{ m}^2 \text{ g}^{-1}$ ), and under copious amounts of water. Surfactants and cationic polyelectrolytes are widely used that together with silicones are the main compounds used nowadays to provide lubrication to hair. In bulk water, these polymers interact with oppositely charged and zwitterionic surfactants. When hair is present, the interactions between these polymers and the surface are essential to eventually help its adsorption.<sup>11,12</sup> Human hairs have complex structures in which each fiber is in



fact a bundle of thinner fibers thus presenting a huge specific area, and in which both absorption and adsorption of polymers and surfactants take place. Moreover, the hair fibers have a chemically heterogeneous structure. To understand the behavior of polymers and surfactants in contact with hair fibers it is important to start with the analysis of relatively simple model systems. A reasonably good model system for understanding the adsorption of polyelectrolytes used in shampoo and conditioner formulations is a negatively charged flat surface. Even though they cannot account for the chemical heterogeneity of surface hair fibers, it is good for comparing the Coulombic and entropic contributions to the adsorption of a set of different polymers frequently used in cosmetics.

Polymer adsorption process is affected by several variables:<sup>1,6</sup> charge densities of the polymer and of the surface,<sup>13</sup> polymer concentration,<sup>14</sup> ionic strength,<sup>15</sup> pH<sup>16</sup> and temperature,<sup>17</sup> as well as solvent quality for the polymer.<sup>18,19</sup> As a consequence, it is important to measure the properties of adsorbed layers (thickness, composition, adsorbed mass, water content, mechanical and tribological properties, etc.). In addition to the above properties, the study of the adsorption kinetics is very important because in real life use shampoos and conditioners are applied during a limited time. As a consequence, it is necessary that the maximum

**Received:** May 25, 2011

**Accepted:** July 12, 2011

**Published:** July 12, 2011

amount of hydrated polymer is adsorbed during the application time. For two different polymers a higher equilibrium adsorption might not necessarily correspond to a higher amount at the practical product application time.<sup>11,12</sup> The adsorption kinetics of polyelectrolytes presents several steps:<sup>4,6,8,12,20</sup> The first one is related to mass transport toward the surface, which may be determined by convection and/or diffusion depending on the experimental conditions. The second one is the attachment of the polymer onto the surface, which depends on the existence of adsorption barriers. Finally, the third stage corresponds to the reconfiguration of the adsorbed molecules that relax from coil to train-loop-tail structure.<sup>4,7,21</sup> However, in most of the cases, the time scales of some of the kinetic steps overlap, thus making difficult to separate them experimentally.<sup>15</sup>

In this work, we have studied the adsorption process of four different polymers onto solid surfaces with different charge densities.<sup>11,22</sup> Taking into account that modern cosmetic formulations contain a variety of neutral and charged polymers,<sup>23</sup> we have studied four water-soluble polymers used in real formulations. Two of them are hydrophilic and neutral: poly(ethyleneglycol), PEG, and poly(vinylpyrrolidone), PVP. The other two are cationic polysaccharides: JR400 and Jaguar C13S. The backbones of the two polysaccharide polyelectrolytes are functionalized with different charged groups that lead to different charge densities. In addition, polysaccharide polymers with different charged groups have different chain rigidities, which strongly affects the adsorption behavior, at least at the air/liquid interface.<sup>24</sup>

The effect of charge density of the polymers on the adsorption onto solid surface has been discussed previously;<sup>1,25–28</sup> however, less attention has been paid to the effect of charge density of the surface on the adsorption process.<sup>21,25</sup> It is known that the driving forces for the adsorption process are polymer–surface interactions, the entropy penalty due to the loss of chain conformations upon adsorption, and the entropy gain due to the release of counterions in the case of charged polymers.<sup>29</sup> The adsorption and the final structure of the layers are controlled by the chemical nature of the polymers and surfaces. The latter characteristics are essential in the action mechanism of several hair treatments whose efficiency depends on the alterations that they produce on the surface nature of the hair (charge, defects, etc.).<sup>30,31</sup>

In this study, we have analyzed the effect of charge density of the surface on the adsorption kinetics, the total adsorbed amount, the mechanical properties, water content, and the driving force of the adsorption process.

## 2. EXPERIMENTAL SECTION

**2.1. Chemicals.** Figure 1 shows the chemical structure of the polymers studied. Neutral hydrophilic polymers, were poly(ethyleneglycol), PEG, and poly(vinylpyrrolidone), PVP. Both polymers were purchased from Merck Chemical Division (Germany) and with molecular weights close to 10 kDa. The polyelectrolytes were two cationic polysaccharides that differ in the number of charged groups per monomer: They are hydroxyethyl cellulose quaternized with 2,3-epoxypropyl-trimethyl-ammonium chloride, JR400, and hydroxypropyl guar trimethyl-ammonium chloride, Jaguar C13S, both from Union Carbide Corp. (USA) and with molecular weights close to 500 kDa. All the polymers were used without further purification.

It is important to notice that the maximum charge in the case of the polysaccharide polymers is imposed by the Manning condensation limits, thus the total charge is not simply  $N$  times  $z$ , where  $N$  is the

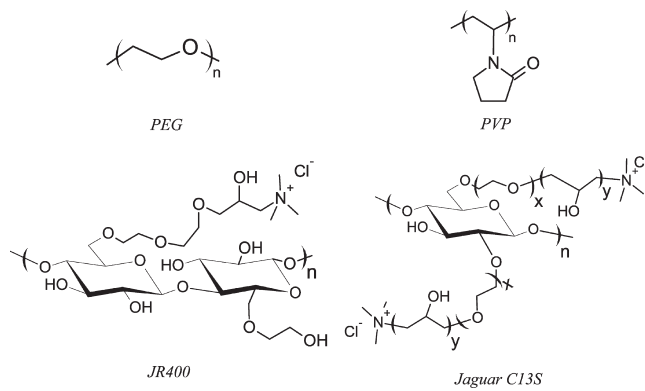


Figure 1. Chemical structures of the polymers used in the study.

number of charged monomers, and  $z$  their charge. Notice that in Figure 1,  $|z| = 1$  for all the charged groups, and that the chemical nature of charged groups is the same. Therefore, even though some local effects might be expected, it seems reasonable to assume that the Manning condensation effects will be the same, or at least very similar within each family of polymers. Therefore, the charge density should be directly related to the average number of charge per monomer.

The water was of Milli-Q quality (Millipore RG model) with a resistivity higher than  $18.2\text{ M}\Omega$  and Total Organic Content lower than 10 ppb. All the experiments were done at  $(298.1 \pm 0.1)\text{ K}$ . The solutions of concentration  $1\text{ mg mL}^{-1}$  were prepared by weight using an analytical balance with a precision of  $\pm 0.01\text{ mg}$ .

**2.2. Substrates.** Prior to the experiments all the substrates used were cleaned with piranha solution ( $70\%$   $\text{H}_2\text{SO}_4$  (conc)/ $30\%$   $\text{H}_2\text{O}_2$  (aq), **Warning: piranha solution is extremely oxidizing**) over a period of 30 min and then thoroughly rinsed with pure water.

For the dissipative quartz-crystal microbalance experiments (D-QCM), quartz crystals (AT-cut, KSV, Finland) with two different surface coating were used as substrate. First, conventional gold coated quartz crystals whose surface was modified with coatings having different charge densities. For this purpose self-assembled monolayers of thiols were built on the surface of the gold electrode. Two different thiols with similar main chain but with different terminal functionalization were used: (a) the sodium salt of 3-mercaptopropanesulfonic acid (charged thiol,  $[\text{Na}^+ \text{HS}-\text{(CH}_2)_3-\text{SO}_3^-]$  Purity =90%, Sigma-Aldrich, Germany), and (b) 1-propanethiol (uncharged thiol,  $[\text{HS}-\text{(CH}_2)_2-\text{CH}_3]$  Purity =98%, Sigma-Aldrich, Germany). Three functionalization levels were investigated: 100% ( $\zeta$ -potential around  $-39 \pm 5\text{ mV}$ ), 50% ( $\zeta$ -potential around  $-26 \pm 3\text{ mV}$ ) and 0%, with reference to the molar ratio between charged and noncharged molecules in the functionalization mixture (0% means that the electrode had monolayers of uncharged thiol only and 100% means that the electrode had monolayers of charged thiol only). A 50% mixture of the two thiols was chosen as to obtain thiol self-assembled monolayers where the molecular segregation between the thiol chains is avoided as reported by Tielens et al.<sup>32</sup> To test the effect of the chemical nature of the charge substrate, we used a second type of electrode to study the adsorption process of the polymers: an electrode coated with silica (KSV, Finland) with  $\zeta$ -potential around  $-42 \pm 3\text{ mV}$ . Negatively charged silicon wafers (Siltronix, France) were used as substrates in the ellipsometry experiments. In this case only one charge density is considered. The surface of the wafers and their charge density are equal to that of the silica coated surface of the QCM electrodes. The values of  $\zeta$ -potential are referred to colloidal particles with the same surface nature and functionalization that the flat surface used in this study. The measurements were made using a Zeta NanoSizer (Malvern Instruments, U.S.A.).

**2.3. Techniques.** A dissipative quartz-crystal microbalance (D-QCM) from KSV (Model QCM Z-500, Finland) was used. The

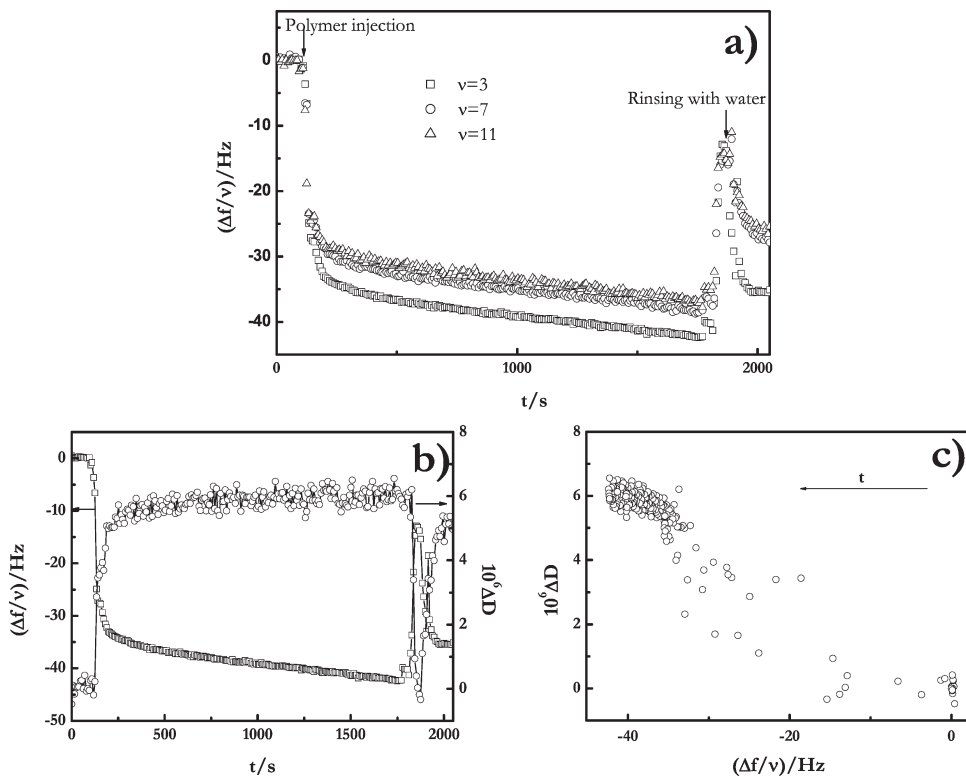


**Figure 2.** Example of a D-QCM experiment. (a) Adsorption kinetics and washout processes for the adsorption of a layer of Jaguar C13S depicted as the time dependence of the shift of the central frequency of the different overtones of the quartz sensors. For clarity only the curves for  $\nu = 3, 7$ , and 11 are shown. (b) Time dependence of the  $\Delta f/\nu$  and the  $\Delta D$  for the third overtone. (c)  $\Delta D$  vs  $\Delta f/\nu$  graph. The experiments correspond to a polymer solution with  $c \approx 1 \text{ mg mL}^{-1}$  adsorbed onto a  $\text{SiO}_2$  surface.

quartz crystals present a characteristic frequency in vacuum  $f_0 = 5 \text{ MHz}$ . D-QCM provided the impedance spectra of the crystal for the fundamental mode, and for odd overtones of the fundamental resonance up to the 11th (central frequency  $f_{11} = 55 \text{ MHz}$ ). For data analysis, we adopted the model proposed by Johannsmann et al.<sup>34,35</sup> that provides the total adsorbed mass (polymer and water) and the shear compliance of the adsorbed layer.

To measure the adsorbed polymer mass, we have carried out ellipsometric experiments. We used an imaging null ellipsometer from Nanofilm (model EP3, Germany), and all the experiments were carried out on a solid–liquid cell at a fixed angle of  $60^\circ$ . The ellipsometric angles  $\Delta$  and  $\Psi$  describe the changes in the state of polarization when the light is reflected at a surface.<sup>36</sup> To obtain the ellipsometric adsorbed mass,  $\Gamma_{\text{opp}}$ , we have used a four-layer model as described in previous works.<sup>19,37</sup>

As will be discussed below, both techniques give complementary information and have to be combined for calculating the amount of water adsorbed together with the polymers.

### 3. RESULTS AND DISCUSSION

**3.1. Adsorption Process.** All the adsorption experiments were performed under static conditions without stirring.<sup>2</sup> As an example, Figure 2 shows the results from a D-QCM experiment for Jaguar C13S adsorbed onto  $\text{SiO}_2$  surface, Figure 2a shows the shift in frequency of the quartz sensor,  $\Delta f$ , normalized by the number of overtone,  $\nu$ , for all the overtones measured (even though  $\nu = 3, 5, 7, 9$ , and 11 were measured, for clarity, only  $\nu = 3, 7$ , and 11 are shown in the figure). Three different stages can be distinguished in Figure 2a: first the frequency of the base crystal

immersed in the solvent is obtained; then a sharp decrease in  $\Delta f/\nu$  is observed when the polymer solution is introduced in the measurement chamber. This decrease in  $\Delta f/\nu$  is due to the adsorption of material on the surface of the sensor; when the adsorption process ends ( $\Delta f/\nu = \text{constant}$ ) the measurement chamber is flushed with the same solvent used in the polymer solution, and at the same temperature of the measurements, in order to remove the chains that are weakly adsorbed to the substrate (third stage). After the rinsing process, small shifts on the frequency may take place. However, these changes on the signal are always much smaller than those observed during the adsorption process and can be attributed to swelling–shrinking process of the adsorbed layers. This confirms that the adsorption process of polymer onto solid surfaces as a quasi-irreversible process, in agreement with previously reported results.<sup>6,19,38,39</sup> Note that during the injection and rinsing processes fast shifts in  $\Delta f/\nu$  were observed that were not taken into account for the analysis of adsorption process.<sup>2</sup> These changes are experimental artifact consequence of the design of the measurement chamber.<sup>40</sup> Similar qualitative trends were observed for the  $\Delta$  and  $\Psi$  ellipsometric angles.

Figure 2a also gives some qualitative insight on the mechanical behavior of the adsorbed films. For purely elastic films (where the Sauerbrey equation is valid),<sup>41</sup> the results of  $\Delta f/\nu$  for all the overtones should collapse onto a single master curve. The lack of overlapping indicates that the adsorbed films behave as a viscoelastic layer.<sup>35</sup> This observation is further confirmed in Figure 2b by the behavior of the dissipation factor,  $D$ , which strongly increases during the adsorption process after a short

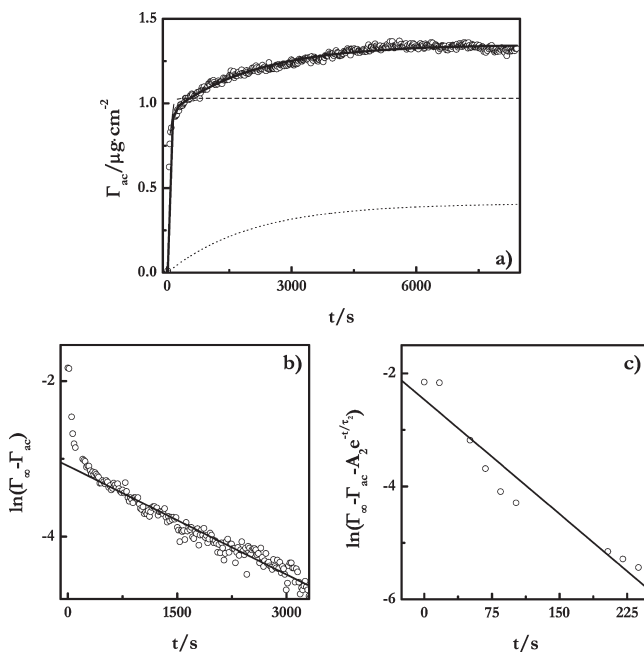


**Figure 3.** Example of adsorption kinetics analysis (D-QCM technique). (a) Adsorption dynamics for a layer of PVP adsorbed onto a total charged substrate from a solution with concentration  $c \approx 1 \text{ mg mL}^{-1}$ . The solid line shows the best fit to the model proposed by Chiang et al.<sup>48,49</sup> The two exponential components are shown: --- fast step and ··· slow step. Notice that approximately 78% of the total adsorbed mass is adsorbed after the fast step. (b) Plot of logarithm of  $(\Gamma_\infty - \Gamma)$  vs time, where  $\Gamma_\infty$  represents the surface concentration at the equilibrium, after long adsorption times where the fastest exponential becomes negligible, it can be fitted to a straight line (solid line). (c) Short time behavior of the adsorption kinetics, a plot of  $\ln(\Gamma_\infty - \Gamma - A_2 e^{-t/\tau^2})$  vs time gives a straight line (solid line).

induction period. Figure 2c shows the relationship between  $\Delta D$  and  $\Delta f/\nu$  suggesting the existence of rearrangements of the preadsorbed chains, which is reflected in the linear or nonlinear trends of the plot,<sup>42</sup> and allows us to obtain qualitative information about energy/entropy balance in the adsorption process.<sup>43,44</sup> High  $\Delta D$  values in this plot indicate that the energetic factors are predominant, while low  $\Delta D$  vs  $\Delta f/\nu$  values indicate that entropy is the factor that controls the adsorption process.

**3.2. Adsorption Kinetics.** The adsorption kinetics is controlled by a complex balance of different forces such as the polymer–solvent and polymer–surface interactions, the decrease of entropy due to the loss of conformations of the polymer chain when it approaches the solid surface, and the release of counterions.<sup>45</sup> Even though there are several theoretical studies in the literature about this topic,<sup>47,8</sup> from the experimental point of view, it is not easy to study the kinetic process in detail,<sup>21,46–49</sup> especially at very short times. Lane et al.<sup>46</sup> studied the adsorption kinetics of sodium salt of poly(4-styrenesulfonate) and poly-[1-[4[(3-carboxy-4-hydroxyphenylazo)benzenesulfonamido]-1,2-ethanediyl sodium salt] on polyelectrolyte multilayers using dual-beam polarization interferometry and D-QCM. They qualitatively explained the adsorption kinetics results by three different processes, which is in accordance with the recent results by Bijelic et al.,<sup>21</sup> and with the brownian dynamics simulations of Linse and Källrot<sup>4</sup> for the adsorption of neutral polymers onto solid surfaces. However, the characteristic times of the two first processes are so close to the experimental time resolution of our

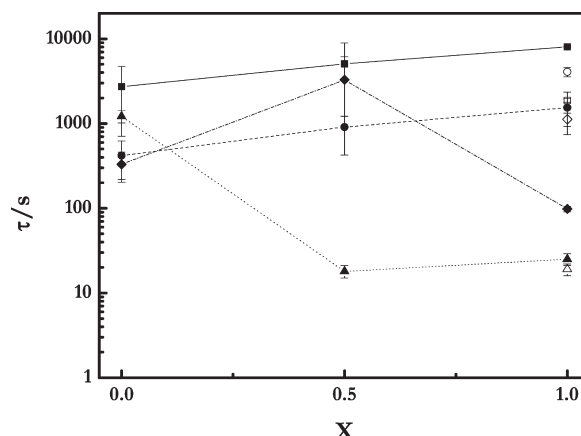


**Figure 4.** Adsorption times of studied polymers on surfaces with different density of charge,  $x$ . The solid symbols represent the adsorption on gold surfaces with self-assembled monolayers having different charge density,  $x$ , (the charge density is expressed as percentage in the assembling of thiols with a charge group), the lines show the general behavior. The open symbols shown in  $x = 1$  represent the adsorption on  $\text{SiO}_2$  surfaces, data obtained with D-QCM. Legend: ■ □ PEG ● ○ PVP ▲ △ JR400 ◆ ◇ Jaguar C13S. The error bars are obtained taking into account the precision of the measurements and the errors introduce by the analysis process.

techniques (7 s in the case of D-QCM experiments and 18 s in the case of ellipsometry experiments)<sup>6</sup> that no physically sound discussion of these values can be done for the fastest kinetic process. Figure 3 shows that the adsorption kinetics may be considered as a bimodal process as proposed by Chiang et al.<sup>50,51</sup> The first fast step may be related to the transport of the chains toward the surface and the initial adsorption, and it must be stressed that this first process is not diffusion controlled, as revealed by the fact that the adsorbed mass does not show a  $t^{1/2}$  dependence, in accordance to the predictions of Cohen-Stuart,<sup>8</sup> and qualitatively might be related to the two first stages of the model of Linse and Källrot.<sup>4</sup> The second slow step might be related to the reorganization of the preadsorbed chains. However, in order to avoid any oversimplification on the analysis of the kinetics results, we only comment here the total adsorption time,  $\tau$ , necessary for the adsorption of different polymers in different experimental conditions (surface charge density, polymer nature, polymer concentration, etc.). Figure 4 summarizes the global adsorption times obtained for the different polymers.

The adsorption times depend on the chemical structure of the polymers. For the hydrophilic neutral polymers (PEG and PVP), the adsorption time slightly increases with charge density of the thiol-coated surface, whereas for the polysaccharide polyelectrolytes (JR400 and Jaguar C13S),  $\tau$  decreases as  $x$  increases. This different behavior is due to the different type of interactions that drive the adsorption process.

The results for the hydrophilic neutral polymers (PEG and PVP) point out that the adsorption process is slower on surfaces with higher charge density. In this case the adsorption is driven by non-electrostatic affinity between the surface and the polymer<sup>1,6,25</sup> since the adsorption rate for PEG and PVP is similar in all the thiol-coated surfaces. In principle, similar values of zeta potential found for silica surfaces and the thiol-coated gold surfaces with  $x = 1$  do not imply that the interaction between the polymers and both surfaces are considered the same. In effect, for silica surfaces, hydrogen-bond interactions between non-charged groups of the

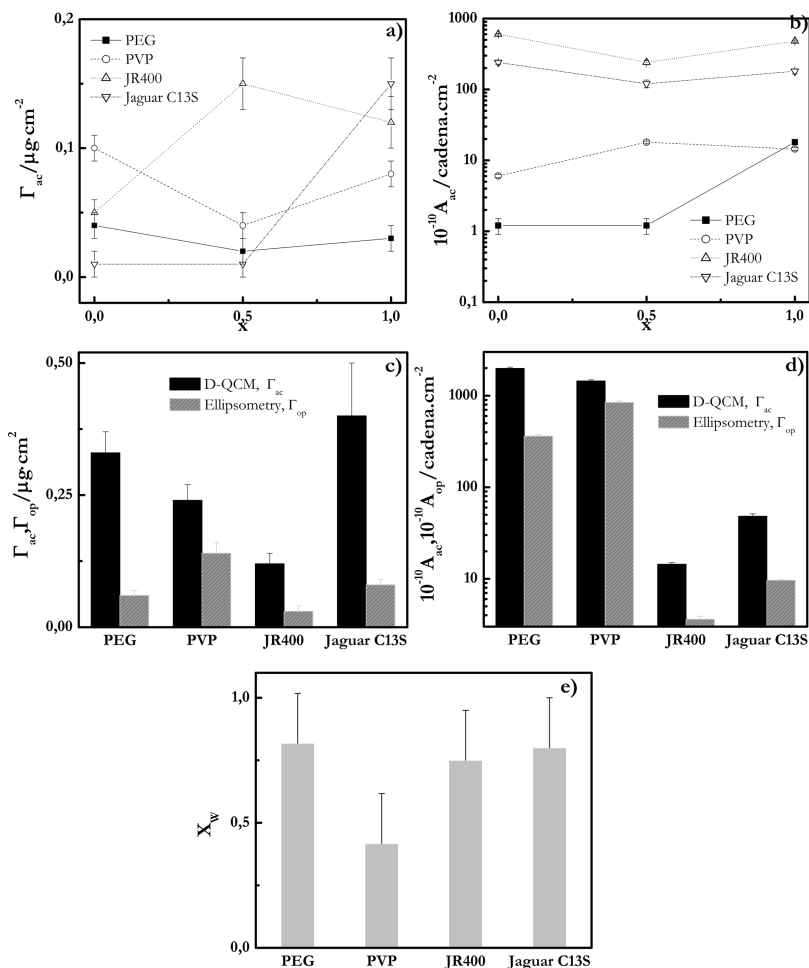


**Figure 5.** (a) Amount of adsorbed material on surfaces with different charge density,  $x$  (the charge density is expressed as percentage of charged thiol in the) for the different polymers studied. All the experiments were made from solutions of  $c \approx 1 \text{ mg mL}^{-1}$ . (b) Surface density of adsorbed chains,  $A_{ac}$ , for the adsorption experiment reported in part a. (c) Comparative  $\Gamma_{ac}$  and  $\Gamma_{op}$  for the layers of the different polymers adsorbed on a surface with similar properties. (d) Surface density of adsorbed chains,  $A_{ac}$  and  $A_{op}$ , for the adsorption experiment reported in part c. (e) Water content for the layer of the different studied polymers. The error bars are obtained taking into account the precision of the measurements and the errors introduce by the analysis process.

polymers and non-dissociated silanol group of the surface may occur.<sup>33</sup> One might expect these interactions to be more important for the neutral polymers than for the polyelectrolytes where Coulombic interactions and counterions release are the main driving forces for adsorption. In fact the adsorption experiments performed on the thiolated-gold and on the silica-coated electrodes have given undistinguishable results. This confirms that any specific interactions between the polymers studied and the silanol groups are of minor importance.<sup>1</sup>

In the case of charged polysaccharide polymers, we found that the adsorption process was controlled by the electrostatic interactions so the adsorption is slowed down as the surface charge density of the substrate decreases. This is due to the essential role of the electrostatic interaction in the adsorption of polyelectrolytes, presenting the hydrophobic interactions a limited influence on the process. It is noticeable that for high charge density of the surface, the adsorption time is lower than 100 s, which indicates that the adsorption of rigid polymers, such as polysaccharides, onto charged surfaces takes place without further reorganization, as in the computer simulations of Linse and Källrot,<sup>4</sup> and in agreement with the flat adsorption of

polysaccharides onto solid surfaces reported by different authors.<sup>52,53</sup> The differences found between JR400 and Jaguar C13S may be explained as resulting from the different charge density of Jaguar C13S (recall that Jaguar C13S holds two charges per unit instead of one per each two units in JR400) that lead to a slowing down of the adsorption as a result of larger electrostatic repulsion than in the case of the adsorption of JR400. The adsorption of JR400 and Jaguar C13S onto silica surfaces presents some clear differences: JR400 shows similar values of  $\tau$  on silica and on charged thiol-surfaces, whereas they are rather different values for Jaguar C13S at  $x = 1$ . Although there is no experimental proof of the physical origin of this behavior, the different chemical structure of the two polysaccharides might change the balance between electrostatic and hydrogen-bond interactions in the case of silica surfaces. The results point out that the adsorption process of polymers onto solid surfaces is the result of a complex balance of affinity between the different components involved on it.

**3.3. Adsorbed Mass and Water Content.** As expected, the adsorbed mass (Figure 5a) depends on both the polymer and on the surface charge density for the two families of polymers studied.<sup>6</sup>

The results obtained for the adsorption of neutral hydrophilic polymer (PVP and PEG) onto surfaces of gold functionalized with thiols having different charge densities (Figure 5a) show that, independently of charge density of the solid surface, the total adsorbed amount is low as a result of the absence of functional group that leads to an effective interaction between the polymers and the surfaces, being the adsorption controlled by the non-electrostatic interactions. However, in the case of adsorption onto a  $\text{SiO}_2$  surface (see Figure 5b), where the interactions may be driven by hydrogen bonds, the adsorption increases abruptly in accordance with the results reported by Olanya et al. for the adsorption of poly(ethylene oxide)-based polymers onto similar surfaces.<sup>33</sup>

For charged polysaccharide polymers (see Figure 5a), the behavior is different, the adsorbed amount increases with the charge density of the surface, and the adsorption onto  $\text{SiO}_2$  is similar to that observed on surfaces with charged thiol (see Figure 5a,b). This gives further support to the idea that the adsorption of these polymers is driven essentially by electrostatic interactions. However, as we commented above in the case of JR 400, the adsorption on charged thiol-coated surfaces is similar to that observed on  $\text{SiO}_2$  surfaces whereas the adsorption of Jaguar C13S onto  $\text{SiO}_2$  surfaces is higher. A possible explanation has been suggested in the previous section. It is important to notice that the differences observed on the adsorbed amounts between polysaccharides and neutral hydrophilic polymers are in qualitative agreement with the values reported in the literature for neutral and charged polymers.<sup>52,54,55</sup>

The adsorption in terms of the chain per unit of area,  $A_{ac}$ , allows us to eliminate the effect of the molecular weight of the polymer. The values obtained (Figure 5b) confirms the existence of a different scenario for the adsorption of polysaccharides and neutral hydrophilic polymers. Polysaccharides show an increase of the chain per unit of area with the increase of the charge density of the surface. This may be rationalized as result of the different affinity for the adsorption onto the surface. For low charge density of the surface, the number of adsorbed chains is limited leading to a small number of chains in a big area, and consequently  $A_{ac}$  is low. Whereas with the increase of the charge density of the surface, the electrostatic interactions start to be important and this leads to the adsorption of a high number of rigid rod chains distributed in the whole surface with the subsequent increase in  $A_{ac}$ . In the case of neutral hydrophilic polymers, independently of the charge density of the surface, the value of  $A_{ac}$  remains almost constant at a high value. This is due to the fact that the chains interact with the surface at a low number of attachment points, with long segments protruding into the water solution.

The comparison between the adsorbed mass obtained from D-QCM,  $\Gamma_{ac}$ , and ellipsometry,  $\Gamma_{op}$ , allowed us to obtain the amount of water associated with the layers using the method introduced for Vörös<sup>56</sup> (see Figure 5e). The water weight fraction,  $X_w$ , in the adsorbed film is given by

$$X_w = \frac{\Gamma_{ac} - \Gamma_{op}}{\Gamma_{ac}} \quad (1)$$

In a previous work, it was shown that this approach gave results in good agreement with the values of  $X_w$  obtained by neutron reflectivity.<sup>19</sup> The results (Figure 5e) show high values of water content in all the adsorbed layers, which suggests that the polymer chains adsorb rather inhomogeneously, forming isolated

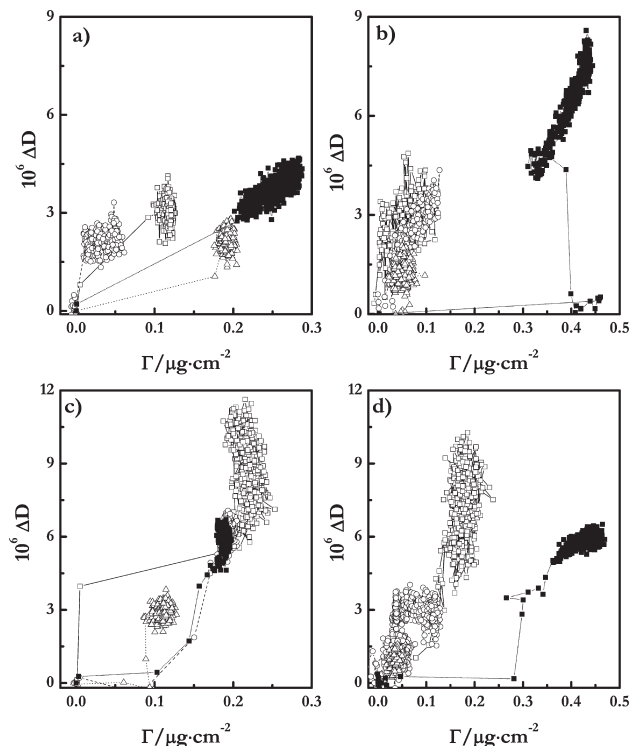


**Figure 6.** Relative entropic contributions, represented as  $\Delta D$  for the third overtone vs  $\Gamma$  obtained for the analysis of the complete impedance spectrum, for the adsorption of different studied polymers. (a) PVP. (b) PEG. (c) JR400. (d) Jaguar C13S. The different symbols indicate different surface. Open symbols indicate adsorption onto thiol surfaces with different charge density:  $\square x = 1$ ,  $\circ x = 0.5$ , and  $\Delta x = 0$ . And solid symbol indicate adsorption onto  $\text{SiO}_2$  surfaces:  $\blacksquare = \text{SiO}_2$ . Note that the use of the dissipation factor obtained for the other overtones do not modified the meaning of the results.

adsorbed coil-like pancakes or filling the whole surface as highly swelled chains. This conclusion is also in agreement with previous results from other groups.<sup>57–59</sup> It is noteworthy that the PVP layers show a significantly different water content, which may be due to the ability of PVP to form hydrogen bonds with the surfaces and with the solvent molecules. The high values of  $X_w$  plasticize the adsorbed films leading to values of the shear modulus close to 1 MPa, similar to the values of polymer gels.

**3.4. Adsorption Driving Force.** The D-QCM technique has allowed us to discuss the entropy contribution to the adsorption process that is due to the loss of conformational freedom of the polymer chains and to the release of counterions into the solution when polymer adsorption takes place.<sup>42–44</sup> Gurdak et al. have shown that an increase in the dissipation factor in a plot of  $\Delta D$  versus the amount of adsorbed material obtained from the analysis of the different overtones,  $\Gamma$ , is associated to a lower weight of the entropy contribution.<sup>61</sup> Note that the entropic/energetic contributions here obtained are established in a relative scale, thus they are only useful for the comparison of the different polymers onto a given substrate. This argument was also used by Ozeki et al. in the analysis of the binding processes of different biopolymers to the quartz crystal sensor.<sup>62</sup> Figure 6 shows the following trends: For the neutral polymers onto thiol-coated surfaces the adsorption is entropy driven, although entropy contribution is much smaller onto silica. In the case of polysaccharides adsorption is energy-driven onto charged surfaces,

while it is entropy-driven onto uncharged surfaces. The different degree of entropic control as function of the nature of the surface may be related to the differences in the structure of the layers: layers with polymeric segments protruding to the solution presents a more important entropic contribution than those with the polymer chains adsorb in a more flat conformation onto the solid substrate.

The differences found for the adsorption onto the different surfaces studied in this work are relevant for cosmetic applications due to the well-known chemical heterogeneity of the hair fibers and of the skin. In effect the physicochemical properties of the surface of hair may change depending on parameters like light, temperature, brushing, or weathering. Natural hair is for example very hydrophobic before any of the processes listed before take place. Ionic groups of the protein (keratin) lying at the surface of the hair fibers are more exposed; the lipid layer present at the surface becomes disrupted, etc. The distribution of these groups play an important role on the way that a polymer may adsorb at their surface, especially if the electrostatic interaction is the main force.<sup>10,11,22</sup>

## 4. CONCLUSIONS

The adsorption behavior of two different kinds of polymers (cationic polysaccharides and neutral hydrophilic polymers) on solid surfaces with different charge density has been studied by D-QCM and ellipsometry. Both techniques indicated that the adsorption process was essentially irreversible. The adsorption kinetics of the polymers appears as a complex process that shows different dependence on the charge density of the surface according to the polymer nature, this behavior being related to the different interactions that take place during the adsorption process. The adsorbed amount depends on the polymer nature (charged or uncharged polymers) and on the charge density of the surface for all the polymers. Additionally, as a result of the interactions involved in the adsorption process, the nature of the charge may affect adsorption. The comparison of adsorbed mass values obtained from D-QCM and ellipsometry allowed us to estimate the water content of the layers. In general, the overall water content is high. The D-QCM allowed us to calculate the complex shear modulus of the film.  $G'$  and  $G''$  show values in the range of a few MPa, which are characteristic of polymer in a rubber-like state. The experimental results show an important contribution of the entropy in the control of the adsorption process of the layers. The differences found for the adsorption onto the different surfaces studied in this work are relevant for cosmetic applications due to the well-known chemical heterogeneity of the hair fibers and of the skin. In these cosmetic substrates, the amount and distribution of chemical groups is known to change depending on previous treatments or because the exposition to external agents that disrupt the protective lipid layer present at the surface. These situations impact the charge distribution at the surface and therefore the subsequent interaction with polyelectrolytes.

## ■ AUTHOR INFORMATION

### Corresponding Author

\*E-mail: rgrubio@quim.ucm.es (R.G.R.); gluengo@rd.loreal.com (G.S.L.).

### Present Addresses

<sup>†</sup>CNR-Istituto per L'Energetica e le Interfasi, Via Marini 6, 16149-Genova, Italy.

## ■ ACKNOWLEDGMENT

The work of the group at Madrid was supported in part in part by MICINN under grant FIS2009-14008-C02-01, by ESA under Grant MAP AO-00-052 (FASES) and PASTA and by EU under MULTIFLOW excellence network of the 7th FP. E.G. was supported by a FPU fellowship from MICINN. The authors are grateful to the UIRC of the CAI of Spectroscopy of Complutense University for the use of the ellipsometer. We thank F. Leroy (L'OREAL) for their support for this project

## ■ REFERENCES

- (1) Holmberg, K.; Jönsson, B.; Kronberg, B.; Lindman, B. *Surfactants and Polymers in Aqueous Solution*; John Wiley & Sons: Chichester, UK, 2002.
- (2) Guzmán, E.; Ritacco, H.; Ortega, F.; Svitova, T.; Radke, C. J.; Rubio, R. G. *J. Phys. Chem. B* **2009**, *113*, 7128–7137.
- (3) Ferri, J. K.; Kotsmar, C.; Miller, R. *Adv. Colloid Interface Sci.* **2010**, *161*, 29–47.
- (4) Linse, P.; Källrot, N. *Macromolecules* **2010**, *43*, 2054–2068.
- (5) Netz, R. R.; Andelman, D. *Phys. Rep.* **2003**, *380*, 1–95.
- (6) Fleer, G. J.; Cohen Stuart, M. A.; Scheutjens, J. M. H. M.; Cosgrove, T.; Vicent, B. *Polymer at Interfaces*; Chapman & Hall: Cambridge, UK, 1993.
- (7) Källrot, N.; Dahlqvist, M.; Linse, P. *Macromolecules* **2009**, *42*, 3641–3649.
- (8) Cohen-Stuart, M. A. *J. Phys.: Condens. Matter* **1997**, *9*, 7767–7783.
- (9) Hubbell, J. A. *Curr. Opin. Biotechnol.* **1999**, *10*, 123–129.
- (10) Baghdadli, N.; Luengo, G. S. *J. Phys.: Conf. Ser.* **2008**, *100*, 052034.
- (11) Faucher, J. A.; Goddard, E. D.; Hannan, R. B. *Text. Res. J.* **1977**, *47*, 616–620.
- (12) Goddard, E. D.; Schmitt, R. L. *Cosm. Toiletries* **1994**, *109*, 55–61.
- (13) Guzmán, E.; San Miguel, V.; Peinado, C.; Ortega, F.; Rubio, R. G. *Langmuir* **2010**, *26*, 11494–11502.
- (14) Saarinen, T.; Österberg, M.; Laine, J. *Colloids Surf., A* **2008**, *330*, 134–142.
- (15) Guzmán, E.; Ortega, F.; Baghdadli, N.; Luengo, G. S.; Rubio, R. G. *Colloids Surf., A* **2010**, *375*, 209–219.
- (16) Zhang, X.; Sun, Y. P.; Gag, M. L.; Kong, X. X.; Shen, J. C. *Macrom. Chem. Phys.* **1996**, *197*, 509–515.
- (17) Salomaki, M.; Vinokurov, I. A.; Kankare, J. *Langmuir* **2005**, *21*, 11232–11240.
- (18) Dubas, S. T.; Schlenoff, J. B. *Macromolecules* **1999**, *32*, 8153.
- (19) Guzmán, E.; Ritacco, H.; Rubio, J. E. F.; Rubio, R. G.; Ortega, F. *Soft Matter* **2009**, *5*, 2130–2142.
- (20) Dupres, V.; Camesano, T.; Langevin, D.; Checco, A.; Guenoun, P. *J. Colloid Interface Sci.* **2004**, *269*, 329–335.
- (21) Bijelic, G.; Shovsky, A.; Varga, I.; Makuska, R.; Claesson, P. M. *J. Colloid Interface Sci.* **2010**, *348*, 189–197.
- (22) Goddard, E. D.; Faucher, J. A.; Scott, R. S.; Turnery, M. E. *J. Soc. Cosm. Chem.* **1975**, *26*, 539–550.
- (23) Flick, E. W. *Cosmetic and Toiletry Formulations*; Noyes Publications/William Andrew Publishing: Norwich, NY, 2001.
- (24) Kleinschmidt, F.; Stutbenrauch, C.; Delacotte, J.; von Klitzing, R.; Langevin, D. *J. Phys. Chem. B* **2009**, *113*, 3972–3980.
- (25) Linse, P.; Claesson, P. M. *Macromolecules* **2009**, *42*, 6310–6318.
- (26) Iruthayaraaj, J.; Olanya, G.; Claesson, P. M. *J. Phys. Chem. C* **2008**, *112*, 15028–15036.
- (27) Naderi, A.; Makuska, R.; Claesson, P. M. *J. Colloid Interface Sci.* **2008**, *323*, 191–202.
- (28) Pettersson, T.; Naderi, A.; Makuska, R.; Claesson, P. M. *Langmuir* **2008**, *24*, 3336–3347.
- (29) Fleer, G. J.; Lyklema, J. *Adsorption From Solution at the Solid/Liquid Interface*; Academic Press: New York, 1983.
- (30) Höss, P.; Dieing, R.; Nörenberg, R.; Pfau, A.; Sander, R. *Int. J. Cosm. Sci.* **2000**, *22*, 1–10.

(31) Mizuno, H.; Luengo, G. S.; Rutland, M. W. *Langmuir* **2010**, *26*, 18909–18915.

(32) Tielens, F.; Humblot, V.; Pradier, C.-M.; Calatayud, M.; Illas, F. *Langmuir* **2009**, *25*, 9980–9985.

(33) Olanya, G.; Iruthayaraj, J.; Poptoshev, E.; Makuska, R.; Vareikis, A.; Claesson, P. M. *Langmuir* **2008**, *24*, 5341–5349.

(34) Johannsmann, D.; Mathauer, K.; Wegner, G.; Knoll, W. *Phys. Rev. B* **1992**, *46*, 7808–7815.

(35) Steinem, C.; Janshoff, A. *Piezoelectric Sensors*; Springer-Verlag: Berlin, 2007.

(36) Azzam, R. M. A.; Bashara, N. M. *Ellipsometry and Polarized Light*; Elsevier: Amsterdam, 1987.

(37) Tompkins, H. G. *A User's Guide to Ellipsometry*; Academic Press: Amsterdam, 1993.

(38) Bodvik, R.; Thormann, E.; Karlson, L.; Claesson, P. M. *Phys. Chem. Chem. Phys.* **2011**, *13*, 4260–4268.

(39) Rojas, O. J.; Ernsson, M.; Neuman, R. D.; Claesson, P. M. *Langmuir* **2002**, *18*, 1604–1612.

(40) Viitala, T.; Hautala, J. T.; Vuorinen, J.; Wiedmer, S. K. *Langmuir* **2007**, *23*, 609–618.

(41) Johannsmann, D. *Macromol. Chem. Phys.* **1999**, *200*, 501–514.

(42) Nejadnik, M. R.; Olsson, A. L. J.; Sharma, P. K.; van der Mei, H. C.; Norde, W.; Busscher, H. J. *Langmuir* **2009**, *25*, 6245–6249.

(43) Gurak, E.; Dupont-Gillain, C.; Booth, J.; Roberts, C. J.; Rouxhet, P. G. *Langmuir* **2005**, *21*, 10684–10692.

(44) Höök, F.; Rodahl, M.; Brzezinski, P.; Kasemo, B. *Langmuir* **1998**, *14*, 729–734.

(45) Jia, L.-C.; Lai, P.-Y. *J. Chem. Phys.* **1996**, *105*, 11319–11325.

(46) Lane, T. J.; Fletcher, W. R.; Gormally, M. V.; Johal, M. S. *Langmuir* **2008**, *24*, 10633–10636.

(47) Guzmán, E.; Ortega, F.; Prolongo, M. G.; Rubio, M. Á.; Rubio, R. G. *J. Mat. Sci. Eng.* **2010**, *4* (No 10), 1–13.

(48) Guzmán, E.; Ritacco, H.; Ortega, F.; Rubio, R. G. *Colloids Surf., A* **2011**.

(49) Guzmán, E.; Cavallo, J. A.; Chuliá-Jordán, R.; Gómez, C.; Strumia, M. C.; Ortega, F.; Rubio, R. G. *Langmuir* **2011**, *27*, 6836–6845.

(50) Chiang, C.-Y.; Starov, V. M.; Lloyd, D. R. *Colloid J.* **1995**, *57*, 715–724.

(51) Chiang, C.-Y.; Starov, V. M.; Hall, M. S.; Lloyd, D. R. *Colloid J.* **1997**, *59*, 236–247.

(52) Kaya, A.; Du, X.; Liu, Z.; Lu, J. W.; Morris, J. R.; Glasser, W. G.; Heinze, T.; Esker, A. R. *Biomacromolecules* **2009**, *10*, 2451–2459.

(53) Wang, J.; Somasundaran, P. *J. Colloid Interface Sci.* **2006**, *293*, 322–332.

(54) Wang, L. M.; Lin, Y.; Su, Z. H. *Soft Matter* **2009**, *5*, 2072–2078.

(55) Pattanayek, S. K.; Juvekar, V. A. *Macromolecules* **2002**, *35*, 9574–9585.

(56) Vörös, J. *Biophys. J.* **2004**, *87*, 553–561.

(57) Bonekamp, B. C.; Van der Schee, H.; Lyklema, J. *Croat. Chem. Acta* **1983**, *56*, 695–704.

(58) Vaccaro, A.; Hierrezuelo, J.; Skarba, M.; Galletto, P.; Kleimann, J.; Borkovec, M. *Langmuir* **2009**, *25*, 4864–4867.

(59) Dodo, S.; Steitz, R.; Laschewsky, A.; von Klitzing, R. *Phys. Chem. Chem. Phys.* **2011**, *13*, 10318–10325.

(60) Ferry, J. D. *Viscoelastic Properties of Polymers*; Wiley: New York, 1980.

(61) Gurdak, E.; Dupont-Gillain, C. C.; Booth, J.; Roberts, C. J.; Rouxhet, P. G. *Langmuir* **2005**, *21*, 10684–10692.

(62) Ozeki, T.; Morita, M.; Yoshimine, H.; Furusawa, H.; Okahata, Y. *Anal. Chem.* **2007**, *79*, 79–88.